JOURNAL OF GUIDANCE, CONTROL, AND DYNAMICS
Vol. 22, No. 3, May–June 1999

Robust Adaptive Control of Store Release Event for Wings with External Stores

Prasad V. N. Gade* and Daniel J. Inman†
Virginia Polytechnic Institute and State University, Blacksburg, Virginia 24061

An adaptive control algorithm is numerically implemented to examine the effectiveness of an online estimation/control scheme for stabilizing the store release of a military aircraft. The adaptive law is based on a gradient method used for parameter estimation and is modified with the algorithms of leakage and dynamic normalization to robustify the adaptation. A linear quadratic control law based on a Luenberger observer is then used to close the loop. An active method of decoupling the wing from store pitch inertia effects for the wing/store flutter suppression problem is proposed. The proposed active decoupler pylon involves the use of a piezoceramic wafer strut as an actuator, which acts as a soft spring between the wing and the store. A two-degree-of-freedom typical section of an airfoil is used to represent the structural model of an F-16 aircraft wing, and the flutter problem is studied in incompressible flow regime, where the circulatory component of the aeroloads is modeled using Jones' approximation to the Theodorsen function. The aerodynamic effects on the store are, however, neglected to make the analysis simple. This study demonstrated the effectiveness of the proposed adaptive control strategy in improving the performance and robustness to sudden variation in store mass, a realistic situation representing the dropping of underwing bombs.

Nomenclature

ab	= distance between elastic center and midchord
b	= semichord length
h	= plunge displacement
i	= $\sqrt{-1}$
$\ell_1 b$	= distance between top of strut to elastic center
$\ell_2 b$	= distance between pivot point to elastic center
m_a	= mass per unit length of the piezoceramic wafer actuator
m_s	= mass of the store
m_w	= mass of the wing
$r_\alpha b$	= radius of gyration of airfoil about elastic center
$r_\theta b$	= radius of gyration of pylon/store about pivot point
s	= Laplace variable
$\bar{s}$	= reduced frequency, bs/U
U	= freestream velocity
u	= actuator output (restoring moment to the store)
$x_\alpha b$	= distance between elastic center and c.g. of wing
$x_\theta b$	= distance between c.g. of store to pivot point
x_1, x_2	= aerodynamic lag states
α	= pitch angle of airfoil
Δ_m	= multiplicative uncertainty transfer function
θ	= pitch angle of store relative to airfoil
ρ	= density of air
τ	= nondimensional time, Ut/b
ω_h	= uncoupled wing bending frequency
ω_α	= uncoupled wing torsional frequency
ω_θ	= uncoupled store pitch frequency

Introduction

MILITARY aircraft are required to carry several combinations of under-wing external stores to accomplish a variety of missions. Rigid mounting of these stores causes the coupling between the first torsional mode and fundamental bending frequency of the wing to occur sooner than for the case of a bare wing. This results in a substantial decrease in flutter speed critical for survivability against antiaircraft guns. Although passive methods, such as structural and mass balance techniques, have claimed to alleviate flutter, the associated added weight generally results in decreased aircraft performance. Moreover, the requirement on the aircraft to carry several combinations of stores makes its implementation practically impossible. The use of semiactive control technology suggested in the past also has its own disadvantages. In particular, the use of hydraulically actuated ailerons for control of store-induced flutter did not gain popularity because of the difficulty in the prediction of counteracting unsteady aerodynamic forces produced by the control surfaces and insufficient hydraulic flow-rate requirements. In the early 1980s, a novel semipassive approach of using a soft-spring pivot mechanism for isolating the wing torsion mode from store pitch inertia effects was experimentally proven to be successful in alleviating flutter. The objective of the current research is to investigate the feasibility of robustifying the decoupler pylon-mounted system using active control technology. Instead of a passive decoupler pylon, a piezoelectric wafer actuator, consisting of a series of thin circular plates with piezoceramics laminated to its opposite sides, is proposed for use as an active decoupling tie between the wing and the store. The major use of a piezoceramic actuator controlled system is the solution it provides to the time-delay problems imposed by hydraulic actuators. Although active control technology also has weight penalties due to actuator mass and electronic hardware, the flexibility it offers in addressing robustness issues via modern dynamic feedback controllers places it at an advantageous position relative to passive methods.

During combat maneuvers of a military aircraft carrying underwing stores, many critical parameters change, which affects the performance of the system and which sometimes may lead to flutter. A particular combat situation is when the aircraft ejects stores (missiles). This is frequently accompanied by simultaneous changes in some or all parameters, such as radius of gyration, location of store center of gravity, aerodynamic center position, etc. An adaptive control algorithm is implemented to study whether the online estimation/ control scheme works well for the present wing/store model. The adaptive controller is designed at subcritical flutter speed with the objective of investigating whether any increase in performance and/or robustness is achieved in the presence of modeling uncertainties, when the system is subjected to sudden change in mass parameter value.

Received March 9, 1998; revision received Nov. 10, 1998; accepted for publication Nov. 13, 1998.

*Graduate Research Assistant, Department of Engineering Science and Mechanics; currently (on contract) Product Development Engineer, Next Generation Controller Systems, DaimlerChrysler Corporation, 800 Chrysler Drive, Auburn Hills, MI 48326. Member AIAA.

†Herrick Endowed Professor, Department of Engineering Science and Mechanics; currently G. R. Goodson Professor, Department of Mechanical Engineering. Associate Fellow AIAA.

Background and Motivation

Flutter can be alleviated by conventional passive schemes or by the more advanced active approaches. Passive methods typically include adding mass ballast, relocating store location spanwise and/or chordwise, or tuning the pylon stiffness characteristics.[1–3] These methods, however, are generally tailored to a specific configuration and fail to accommodate different store mass and location combinations.

Active methods, on the other hand, are relatively more flexible and require mere change of control law to accommodate different store combinations. One of the earliest known works on the feasibility of using active control for wing/store flutter suppression was reported by Triplett[4] in 1972. His analytical study of an F-4 Phantom aircraft wing/store configuration involved deflecting ailerons in a manner to produce aerodynamic forces that opposed the flutter causing aerodynamic forces. A number of other investigators made important contributions to the field of active wing/store flutter suppression.[5,6] In 1979, Harvey et al.[7] investigated the feasibility of using adaptive control for wing/store flutter suppression with the Triplett[4] approach. Some researchers[8,9] proposed a slightly modified version that involved feeding back signals from the accelerometers at the fore and aft end of the store to electro–hydraulic actuators to drive vanes attached to the forward part of the store. The deflected vanes generated counteracting aerodynamic forces that stabilized the store pitch motion. Hönlinger and Destuynder[10] used a linear quadratic regulator (LQR) control law to test the described procedure on a Phantom F-4F wing/store configuration. The effectiveness of these methods, however, depended largely on the accurate knowledge of counteracting unsteady aerodynamic forces produced by the control surfaces. This poses a particular problem especially in the transonic range, where the theoretical predictions of the unsteady aerodynamic coefficients of the control surfaces are least reliable.[11]

Triplett's feasibility study[4] in 1972 gained interest in the aeronautical community and was soon followed by an Air Force contract to evaluate the ability of a single wing/store flutter control scheme that would be robust to several different store configurations.[12] Instead of using the control surface's unsteady aerodynamics as in the earlier active methods, Triplett and his colleagues proposed to use a hydraulic actuator to decouple the store vibratory motion from that of the wing. Although the dynamic behavior of this scheme worked quite well in restoring bare wing flutter speed, the actuator's inability to meet high-flow-rate requirements for the control of higher frequency perturbations restricted its practical implementation.

Instead of looking at actuating control surfaces for wing/store flutter suppression, Reed et al.[11] in 1980 argued that the issue should be addressed by looking at the more fundamental cause of flutter, i.e., the coupling between the bending and torsional mode of the wing/store system. They proposed a modified version of the earlier approach. Instead of using a hydraulic actuator as a load carrying tie, a passive soft-spring/damper combination was used together with a low-power active control system to maintain store alignment.

Their idea is based on the argument that, instead of modifying the aerodynamic forces, the frequencies associated with flutter critical bending and torsion modes can be separated by making the wing insensitive to store pitch inertia and can eventually alleviate the adverse coupling to a higher flutter speed. Some researchers[13–17] analyzed this concept and successfully demonstrated its use in wing/store bending–torsion flutter suppression. The bending–torsion flutter involves coupling or the coalescence of bending and torsion mode frequencies as the flutter speed is approached. The frequencies at zero airspeed are those due to the undamped inertially coupled bending and torsion motions. These are slightly reduced from their natural values due to the apparent additional mass term associated with the noncirculatory component of the aerodynamic loads. Because the decoupler pylon isolates the wing from the influence of store pitch inertia, the wing torsion frequency with the decoupled store is substantially higher than that for the wing with the rigidly attached store. As the flight speed is increased, the bending branch frequency remains approximately equal to its ground frequency, while torsion branch frequency decreases from its decoupled ground frequency to a frequency where both branches comes close to one another. These branches do not, however, coalesce because of the presence of aerodynamic damping present in the system.

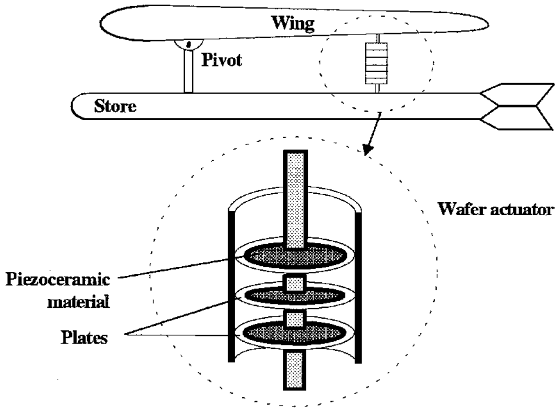

Fig. 1 Wing/store piezostrut arrangement.

The design of a decoupler pylon-mounted store consists of a pitch-pivot mechanism near the fore end that allows the store to pitch relative to the wing surface. Near the aft end, a soft spring is used to decouple the influence of store pitch inertia on wing torsion modes. A low-frequency feedback control is used to prevent large static deflections and maintain alignment. The result is a substantial increase in flutter speed, well beyond that of the bare wing. Based on a feasibility study,[18] a decoupler pylon was fabricated by Clayton et al.[19] and was later successfully implemented on an F-16 aircraft to increase the flutter speed. Instead of using passive soft-spring/damper elements as in Ref. 11 to demonstrate the concept, the current approach proposes an active decoupler pylon for the control of wing/store flutter suppression. The proposed active isolation scheme, shown in Fig. 1, serves two purposes. First, it decouples the wing dynamics from the store pitch inertia effects, a primary source for bending–torsion flutter in wing with external stores. Second, with the aid of a robust controller, it acts as an actuator that stabilizes and maintains the performance characteristics of the closed-loop system in the face of uncertainties at flutter speed. The active pylon consists of a strut with series of thin circular plates laminated on opposite faces with piezoceramic material. The poled directions of the piezoceramics are aligned so that a voltage (control input) applied across the element contracts on one side and expands on the other. The plate bending is then translated into an axial motion along the strut. The piezostrut is designed such that its equivalent stiffness satisfies the criterion of Reed et al.[11] of a soft spring system for isolation purposes, i.e., the store pitch to wing bending frequency ratio should always be less than 1 for effective store flutter alleviation. The novelty in this approach is the use of the strut as both a passive isolator as well as an active actuator to maintain stability and performance. The current active concept has two major advantages over other passive schemes.[11,18,19] Not only does the active decoupler make the system more robust to various uncertainties,[20] but it also has significant weight benefits because it does away with all of the hardware that is required with pneumatic springs and hydraulic dashpots. Moreover, compared to that of a hydraulic actuator, the wafer actuator's faster time response to input command signals makes it suitable for the store flutter suppression problem.

It is proposed that this device will represent a significant improvement in the much needed stroke length requirement over the traditional stack actuator,[21] which has been shown to fail in providing the much needed stroke length for restoring the bare wing flutter speed. Moreover, these actuators typically fail in tension because of the brittle nature of the piezoceramic materials. On the other hand, the current bender-element-type actuator, initially fabricated and designed[22] for use in a large flexible structure, behaves the same both in tension and in compression. Several issues pertaining to the actuator are yet to be quantified, such as actuator dynamics, its time response to input command signals relative to hydraulic actuators, stroke length capability over traditional stack actuators, and power requirements. At the time of writing this paper, the dynamics of the actuator had not yet been identified and, hence, are not included.

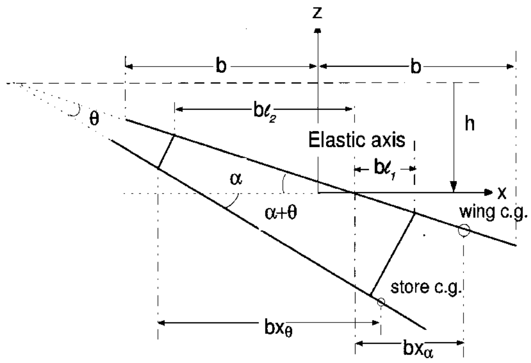

Fig. 2 Schematic of a thin airfoil and decoupler pylon-mounted store.

Therefore, the approach taken here is to lump the actuator dynamics into the uncertainty model.

Plant Description

The analytical model is restricted to a typical section of a thin airfoil with an underwing external store in two-dimensional incompressible flow. The typical section, together with the decoupler pylon and the store, is shown in Fig. 2. The plunging or bending motion of the entire airfoil/store combination together with pitch angles of the lifting surface, α, and of the store, θ, measured relative to the undeformed wing constitute the three degrees of freedom of the wing/store model. Linear and torsional springs at the elastic center are used to model the restraining forces generated by the vertical and angular displacements of the airfoil, whereas restraint to the pitching motion of the store is provided by the decoupler pylon mechanism. Standard sign conventions are used in which the plunging displacement is measured positive downward, whereas a nose-up position of the structure implies a positive pitching angle. The total lift on the airfoil is defined positive up, whereas the pitching moment of the entire airfoil about the one-quarter-chord length point is positive in the nose-up sense. Assuming no structural damping, the equations of motion in the Laplace domain are given by

$$\left(\boldsymbol{M}_s s^2 + \boldsymbol{K}_s\right)\boldsymbol{q}(s) = \begin{Bmatrix} -L_a \\ M_a \\ 0 \end{Bmatrix} + \begin{Bmatrix} Q_h \\ Q_\alpha \\ Q_\theta \end{Bmatrix} \tag{1}$$

where

$$\boldsymbol{q}(s) = \{h/b \quad \alpha \quad \theta\}^T$$

is a vector of generalized coordinates in which the plunge motion h of the airfoil is nondimensionalized by its semichord length b to enable easy comparison with the pitching motions. The left-hand side of Eq. (1) consists of the mass and elastic terms of the airfoil, the actuator, and the attached store, and are given as

$$\boldsymbol{M}_s = \begin{bmatrix} \mu_w + \mu_s + \mu_a & \mu_w x_\alpha + \mu_s(x_\theta - \ell_2) + \mu_a \ell_1 & \mu_s x_\theta + \frac{1}{2}\mu_a \ell_1 \\ \mu_w x_\alpha + \mu_s(x_\theta - \ell_2) + \mu_a \ell_1 & \mu_w r_\alpha^2 + \mu_s\left(r_\theta^2 + \ell_2^2 - 2x_\theta \ell_2\right) + \mu_a \ell_1^2 & \mu_s\left(r_\theta^2 - x_\theta \ell_2\right) + \frac{1}{2}\mu_a \ell_1^2 \\ \mu_s x_\theta + \frac{1}{2}\mu_a \ell_1 & \mu_s\left(r_\theta^2 - x_\theta \ell_2\right) + \frac{1}{2}\mu_a \ell_1^2 & \mu_s r_\theta^2 + \frac{1}{3}\mu_a \ell_1^2 \end{bmatrix}$$

$$\boldsymbol{K}_s = \begin{bmatrix} \mu_w \omega_h^2 & 0 & 0 \\ 0 & \mu_w r_\alpha^2 \omega_\alpha^2 & 0 \\ 0 & 0 & \mu_s r_\theta^2 \omega_\theta^2 \end{bmatrix} \tag{2}$$

where $\mu_w = m_w/\pi\rho b^2$, $\mu_s = m_s/\pi\rho b^2$, and $\mu_a = m_a \ell_a/\pi\rho b^2$ are the virtual masses of the wing, the store, and the actuator, respectively. The terms on the right-hand side of Eq. (1) correspond to the aerodynamics identified as the lift L_a and the moment M_a. A method for calculating the aerodynamic loads due to simple harmonic oscillations of a wing section in incompressible flow was first given by Theodorsen.[23] The theory was then extended to arbitrary motions by Edwards.[24] His generalized unsteady aerodynamic theory divides the aerodynamic loads into noncirculatory and circulatory parts and are expressed in Laplace domain as

$$\begin{Bmatrix} -L_a \\ M_a \\ 0 \end{Bmatrix} = \Big[\underbrace{-s^2\boldsymbol{M}_{nc} - s\boldsymbol{C}_{nc}}_{\text{noncirculatory}} + \underbrace{T(\bar{s})(s\boldsymbol{C}_c + \boldsymbol{K}_c)}_{\text{circulatory}}\Big]\boldsymbol{q}(s) \tag{3}$$

where $\boldsymbol{M}_{nc}$ and $\boldsymbol{C}_{nc}$ are apparent additional mass and damping matrices due to noncirculatory oscillations of the aerodynamic loads given by

$$\boldsymbol{M}_{nc} = \begin{bmatrix} 1 & -a & 0 \\ -a & a^2 + \frac{1}{8} & 0 \\ 0 & 0 & 0 \end{bmatrix}, \qquad \boldsymbol{C}_{nc} = \frac{U}{b}\begin{bmatrix} 0 & 1 & 0 \\ 0 & \frac{1}{8} - a & 0 \\ 0 & 0 & 0 \end{bmatrix} \tag{4}$$

Matrices $\boldsymbol{C}_c$ and $\boldsymbol{K}_c$ correspond to the circulatory part, which are further subdivided into

$$T(\bar{s})[s\boldsymbol{C}_c + \boldsymbol{K}_c] = T(\bar{s})\boldsymbol{R}[s\boldsymbol{S}_2 + \boldsymbol{S}_1] \tag{5}$$

where

$$\boldsymbol{R} = \begin{bmatrix} -2 \\ 2(a + 0.5) \\ 0 \end{bmatrix}, \qquad \boldsymbol{S}_1 = [0 \quad 1 \quad 0]$$

$$\boldsymbol{S}_2 = [1 \quad 0.5 - a \quad 0]$$

In Eq. (5), $T(\bar{s})$ is the complex Theodorsen function, where $\bar{s} = b\omega i/U$ is a Laplace operator associated with nondimensional time Ut/b. The effects of aerodynamics on the store are, however, neglected to make the analysis simpler. With the aid of multivariable robust control techniques, the influence of unmodeled dynamics on the stability and nominal performance of the wing/store flutter suppression system are evaluated in the following. The complete equation of motions is recast into the form

$$\left(\boldsymbol{M}_s s^2 + \boldsymbol{K}_s\right)\boldsymbol{q}(s) = \Big[\underbrace{-s^2\boldsymbol{M}_{nc} - s\boldsymbol{C}_{nc}}_{\text{noncirculatory}} + \underbrace{T(\bar{s})\boldsymbol{R}(s\boldsymbol{S}_2 + \boldsymbol{S}_1)}_{\text{circulatory}}\Big]\boldsymbol{q}(s) + \boldsymbol{H}u(s) \tag{6}$$

where the term u is the actuator input (control moment to the store) acting through the input matrix $\boldsymbol{H} = [0 \ 0 \ 1]^T$ due to the components of the generalized actuator forces and moments Q_h, Q_α, and Q_θ given in Eq. (1). To complete the model in the Laplace domain, Jones's[25] second-order rational approximation to the complex Theodorsen function is used and is given by

$$T(\bar{s}) = \frac{0.5(sb/U)^2 + 0.2808(sb/U) + 0.01365}{(sb/U)^2 + 0.3455(sb/U) + 0.01365} \tag{7}$$

A nonunique state-space representation of Jones's approximation for unsteady circulatory aerodynamic loads can be obtained as

$$\left[\begin{array}{c|c} \boldsymbol{A}_2 & \boldsymbol{B}_2 \\ \hline \boldsymbol{C}_2 & \boldsymbol{D}_2 \end{array}\right] = \left[\begin{array}{cc|c} -0.3(U/b) & 0 & -1.2650(U/b) \\ 0 & -0.0455(U/b) & -0.4927(U/b) \\ \hline -0.0799 & -0.0151 & 0.5 \end{array}\right] \tag{8}$$

The state-space representation of the structural equations and noncirculatory components of the aerodynamic loads is given as

$$\left[\begin{array}{c|c} \boldsymbol{A}_1 & \boldsymbol{B}_1 \\ \hline \boldsymbol{C}_1 & \boldsymbol{D}_1 \end{array}\right] = \left[\begin{array}{cc|c} 0 & I & 0 \\ -(M_s + M_{nc})^{-1} K_s & -(M_s + M_{nc})^{-1} C_{nc} & (M_s + M_{nc})^{-1} R \\ \hline (U/b)^2 S_1 & (U/b) S_2 & 0 \end{array}\right] \tag{9}$$

From Eq. (8) it is evident that the circulatory aerodynamic loads introduce two additional states, called the aerodynamic lags (x_1, x_2), which increase the total number of states to eight. The state-space representation of the augmented system is given by

$$\dot{\boldsymbol{x}} = \boldsymbol{A}\boldsymbol{x} + \boldsymbol{B}u + \boldsymbol{\Gamma}\boldsymbol{w}$$
$$\boldsymbol{y} = \boldsymbol{C}\boldsymbol{x} + \boldsymbol{D}u \tag{10}$$

where

$$\boldsymbol{x} = \{h/b \quad \alpha \quad \theta \quad \dot{h}/b \quad \dot{\alpha} \quad \dot{\theta} \quad x_1 \quad x_2\}^T$$

and

$$\left[\begin{array}{c|c} \boldsymbol{A} & \boldsymbol{B} \\ \hline \boldsymbol{\Gamma}^T & \boldsymbol{D} \end{array}\right] = \left[\begin{array}{cc|c} \boldsymbol{A}_1 + \boldsymbol{B}_1\boldsymbol{D}_2\boldsymbol{C}_1 & \boldsymbol{B}_1\boldsymbol{C}_2 & \boldsymbol{B}_0 \\ \boldsymbol{B}_2\boldsymbol{C}_1 & \boldsymbol{A}_2 & \boldsymbol{0} \\ \hline \boldsymbol{E} & \boldsymbol{0} & \boldsymbol{0} \end{array}\right]$$

where $\boldsymbol{B}_0 = [\boldsymbol{0} \ (\boldsymbol{M}_s + \boldsymbol{M}_{nc})^{-1}\boldsymbol{H}]^T$ and $\boldsymbol{E} = [\boldsymbol{0} \ (\boldsymbol{M}_s + \boldsymbol{M}_{nc})^{-1}\boldsymbol{F}]^T$. The three primary outputs of interest are the plunging motion h, the wing pitch α, and the store pitch angle θ.

Uncertainty Representation

The dynamics of any physical system can never be captured completely by mathematical models. There are always errors associated with the approximations made during the modeling process. These approximations are made either because of the lack of complete knowledge of the system or because of the difficulty in modeling. For instance, the plant described in the preceding section does not include actuator dynamics, and aeroloads on the store are neglected. These imprecisions in high-frequency dynamics are termed as unstructured uncertainties that generally result in an underestimation of the system order. Some of the other examples of unstructured uncertainties for the wing/store flutter problem are the errors from ignoring rigid-body modes of the aircraft.

Uncertainties can also be parametric in nature, where the parameters fluctuate slowly between known values. These low-frequency perturbations are called structured uncertainties. In the case of wing/store flutter problem, they are common in situations of combat when center of gravity location and radius of gyration of the store vary with various rigid-body maneuvers. Hence, during the design of an appropriate controller, the robustness of the closed-loop system in the face of these uncertainties and maintenance of its nominal performance are, therefore, the primary objectives of any control strategy.

In robust control literature, the mathematical representation of uncertainties caused by such unintentional exclusion of high-frequency dynamics generally takes many forms,[26] of which the most commonly used is the multiplicative uncertainty model. Depending on where the errors are reflected with respect to the plant, they are further classified into input and output multiplicative uncertainties. In a narrow sense, using these equivalent input and output multiplicative uncertainties implies an imperfect set of actuators and sensors, respectively. In a broader sense, any plant uncertainty can be referred to by its input or output. This is because the source of unstructured uncertainties is not generally known, and therefore an equivalent input or output uncertainty can be used to characterize the total plant uncertainty.

If $\Delta_m(s)$ represents a proper and stable approximation transfer function error, then the plant transfer function $[Q(s)]$ from u to y_1 (Fig. 3) perturbed with an input multiplicative uncertainty model is given by

$$Q^*(s) = Q(s)[1 + \Delta_m(s)] \tag{11}$$

For simulation and analysis purposes, an approximate model of uncertainty is constructed based on the error from neglecting store aerodynamics.

It is derived based on the argument that had the store aerodynamics been included, then the circulatory aerodynamics of wing and store combination [as opposed to that of the wing alone as in Eq. (5)] can be approximated by Eq. (5), with the exception that the Jones's rational function be replaced by some similar transfer function that closely captures the circulatory effects due to wing/store combination aerodynamics. In other words, the uncertainty in store aerodynamics is reflected on to the uncertainty in Jones's rational function approximation. For simulation purposes, it is assumed that the Jones's approximation $[T(\bar{s})]$ be replaced with a similar rational approximation $[T^*(\bar{s})]$, whose frequency response characteristics are shown in Fig. 4, where

$$T^*(\bar{s}) = \frac{0.5(sb/U)^2 + 0.3398(sb/U) + 0.013627}{(sb/U)^2 + 0.3455(sb/U) + 0.01365} \tag{12}$$

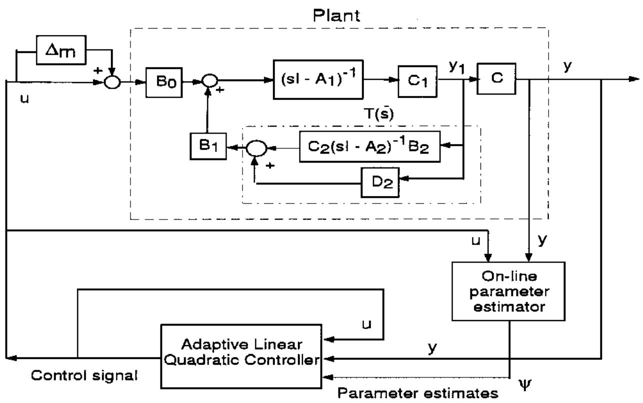

Fig. 3 Block diagram of active flutter suppression.

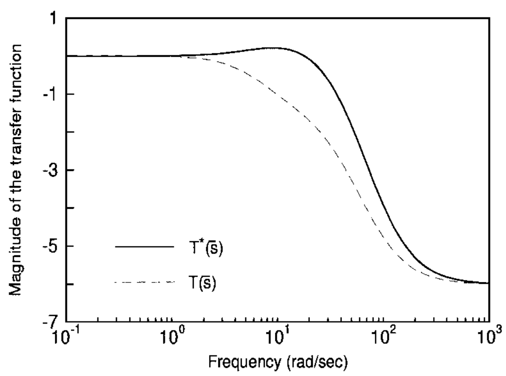

Fig. 4 Jones's approximations.

It is assumed that the majority of the differences between the magnitudes occur in the mid- to high-frequency range. It is to be noted that $T^*(\bar{s})$ is picked only for simulation purposes and lacks any physical backing. However, the motivating argument still remains valid. That is, some other rational function may replace the Jones's approximation that closely represents the circulatory aeroloads around wing–store combination. The aim here is to construct an approximate uncertainty model $\Delta_m(s)$ to reflect the error in store aerodynamics that is later used to perturb the closed-loop system to evaluate for its robustness to modeling limitations. The following details the construction of an uncertainty model $\Delta_m(s)$ from the block diagram shown in Fig. 3.

This block diagram reiterates that flutter is a self-excited phenomenon occurring primarily due to the circulatory aerodynamic loads being regeneratively fed back into the system. Using the Jones's approximation to the Theodorsen's function, the transfer function from u to y_1 can be represented as

$$Q(s) = \frac{\boldsymbol{C}_1(s\boldsymbol{I} - \boldsymbol{A}_1)^{-1}\boldsymbol{B}_0}{1 - \boldsymbol{C}_1(s\boldsymbol{I} - \boldsymbol{A}_1)^{-1}\boldsymbol{B}_1 T(\bar{s})} = \frac{N_0(s)/M(s)}{1 - T(\bar{s})N_1(s)/M(s)} \tag{13}$$

Let the actual plant's transfer function (obtained by using approximations like those of Jones) be given by

$$Q^*(s) = \frac{\boldsymbol{C}_1(s\boldsymbol{I} - \boldsymbol{A}_1)^{-1}\boldsymbol{B}_0}{1 - \boldsymbol{C}_1(s\boldsymbol{I} - \boldsymbol{A}_1)^{-1}\boldsymbol{B}_1 T^*(\bar{s})} = \frac{N_0(s)/M(s)}{1 - T^*(\bar{s})N_1(s)/M(s)} \tag{14}$$

Using the input multiplicative uncertainty, the true plant can be expressed in terms of the nominal plant as

$$\frac{N_0(s)}{M(s) - N_1(s)T^*(\bar{s})} = \frac{N_0(s)}{M(s) - N_1(s)T(\bar{s})}[1 + \Delta_m(s)] \tag{15}$$

The uncertainty model $\Delta_m(s)$ can now be written as

$$\Delta_m(s) = \frac{N_1(s)[T^*(\bar{s}) - T(\bar{s})]}{M(s) - N_1(s)T^*(\bar{s})} \tag{16}$$

which remains the same when an output multiplicative uncertainty model is considered. Because the control theory[26] requires that $\Delta_m(s)$ be stable, the uncertainty model is designed at a flight speed of $0.9U_f$, which is in the subcritical flutter region.

Robust Self-Tuning Regulator

In this work, a continuous-time nonlinear indirect autoadaptive feedback control design is undertaken for the performance enhancement and stability robustification of the wing/store flutter suppression problem. It is assumed that controller parameters and control law are designed based on estimated plant (linear) parameters defined by the polynomial coefficients of the single-input/single-output system (Fig. 3). This type of adaptive control method is also known as a self-tuning regulator technique. An adaptive law based on the gradient method is used for parameter estimation and is modified with the algorithms of leakage and dynamic normalization to robustify the adaptation. The reader is referred to Refs. 27 and 28 for excellent discussion and analytical proofs on these modifications.

Plant Parametrization

With the output taken to be a linear combination of the three primary degrees of freedom equally weighted, the system is represented in a transfer function form as

$$y = \frac{Z}{R}(1 + \Delta_m)u = \frac{b_6 s^6 + b_5 s^5 + \cdots + b_1 s + b_0}{s^8 + a_7 s^7 + \cdots + a_1 s + a_0}(1 + \Delta_m)u \tag{17}$$

which has a relative degree of 2. A common approach to represent such single-input/single-output model for parameter estimation and control applications is the linear parametrization form, where the unknown parameters are separated from the available signals and expressed as

$$\frac{s^8}{\Lambda(s)}y = [b_6, b_5, \ldots, b_0, a_7, \ldots, a_1, a_0]\left[\frac{\boldsymbol{\alpha}_i^T(s)}{\Lambda(s)}u, -\frac{\boldsymbol{\alpha}_i^T(s)}{\Lambda(s)}y\right] + \frac{[b_6, b_5, \ldots, b_0]\boldsymbol{\alpha}_{i-1}^T(s)}{\Lambda(s)}\Delta_m(s)u \tag{18}$$

where $\Lambda(s) = (s + \lambda_f)^8$, $\lambda_f > 0$, and $\boldsymbol{\alpha}_i^T(s) = [s^i, s^{i-1}, \ldots, 1]$, $i = 7$. Here an eighth-order stable filter $1/\Lambda(s)$ is introduced to avoid the use of derivatives of the only available signals, u and y. In notational form, Eq. (18) is written as

$$z = \boldsymbol{\psi}^T\boldsymbol{\phi} + \eta \tag{19}$$

where the signal z constitutes the eighth derivative of the output filtered by $(s + \lambda_f)^8$, $\boldsymbol{\psi}$ is a vector of all unknown parameters, $\boldsymbol{\phi}$ consists of all measurable signals, and η is the disturbance term due to modeling error.

Dynamic Normalization

In this modification, the input and output signals are normalized via the normalized estimation error[27] defined as

$$\epsilon = (z - \hat{z})/m^2 \tag{20}$$

where $m^2 = 1 + n_s^2$ and $n_s^2 = m_n$ is the dynamic normalizing signal designed so that $\boldsymbol{\phi}/m$ and the modeling error term η/m is always bounded. This allows the designer the freedom of not having the plant input signal bounded a priori. The normalizing signal is generated from the differential equation

$$\dot{m}_n = -\delta_0 m_n + u^2 + y^2, \qquad m_n(0) = 0 \tag{21}$$

Another advantage of normalization is that the unbounded modeling error term can be considered as a bounded input disturbance to the adaptive law for which an adaptive control law can then be designed and analyzed at relative ease. Applying gradient method on an instantaneous quadratic cost function $J(\boldsymbol{\psi}) = (z - \boldsymbol{\psi}^T\boldsymbol{\phi})^2/2m^2$, the minimizing trajectory governing the adaptive law is generated by

$$\dot{\boldsymbol{\psi}} = \boldsymbol{\Gamma}\epsilon\boldsymbol{\phi} \tag{22}$$

where $\boldsymbol{\Gamma} = \boldsymbol{\Gamma}^T > \boldsymbol{0}$ is the adaptation gain or the weighting matrix used to control the rate of convergence of various parameters.

Leakage

In the absence of a persistently exciting signal, a bounded input disturbance, such as the one due to the normalized modeling error, may generally cause parameter estimates to drift to infinity with time. Moreover in the presence of an adaptive control law, high-gain feedback generally excites unmodeled dynamics and leads to unbounded plant states. Increasing the adaptation gain $\boldsymbol{\Gamma}$ too much also causes excitation of the high-frequency unmodeled dynamics. To avoid parameter drift and high-gain instability, the original integrator in the adaptation law of Eq. (22) is modified[27] to include an additional term giving it the property of a low-pass filter:

$$\dot{\boldsymbol{\psi}} = \boldsymbol{\Gamma}\epsilon\boldsymbol{\phi} - \boldsymbol{\Gamma}w\boldsymbol{\psi} \tag{23}$$

The idea of modifying the adaptive law is to make the time derivative of the Lyapunov function (used to analyze the adaptive scheme) negative whenever parameter estimates exceeds certain bounds. The choice of w is governed by a continuous switching-σ modification

$$w(t) = \sigma_s = \begin{cases} 0 & \text{if} \quad |\boldsymbol{\psi}(t)| < M_0 \\ \sigma_0\left[\dfrac{|\boldsymbol{\psi}(t)|}{M_0} - 1\right] & \text{if} \quad M_0 \le |\boldsymbol{\psi}(t)| \le 2M_0 \\ \sigma_0 & \text{if} \quad |\boldsymbol{\psi}(t)| > 2M_0 \end{cases} \tag{24}$$

where $\sigma_0 > 0$ is a small constant and M_0 is an upper bound for the unknowns $|\boldsymbol{\psi}|$. The idea behind the switching algorithm is that whenever estimated parameters exceed a certain bound dictated by M_0, the pure integral is converted to a leaky one, and if the estimated parameters are within the threshold bound, then the switching is turned off.

Linear Quadratic Adaptive Controller

Here an adaptive LQR design with an on-line state observer is used for the control law. At each frozen time t, the information from the output, input, and the estimated parameters generated by the adaptive law are used for the purpose. The certainty equivalence approach is assumed wherein the unknown polynomial coefficients are replaced by their estimates. Using the famous separation principle, these estimated parameters are then used to solve the algebraic Riccati equation (ARE) online and for the design of a full-order Luenberger observer, independently.

Because this is a regulator problem, the state-space realization in the observer canonical form is given by

$$\dot{\hat{\boldsymbol{e}}} = \hat{\boldsymbol{A}}\hat{\boldsymbol{e}} + \hat{\boldsymbol{B}}u - \hat{\boldsymbol{K}}_0(\boldsymbol{C}^T\hat{\boldsymbol{e}} - y) \tag{25}$$

where

$$\hat{\boldsymbol{A}} = \begin{bmatrix} -\hat{a}_7 & 1 & 0 & \cdots & \cdots & 0 \\ -\hat{a}_6 & 0 & 1 & \cdots & \cdots & 0 \\ \vdots & \vdots & \vdots & \ddots & \vdots & \vdots \\ -\hat{a}_0 & 0 & 0 & \cdots & \cdots & 1 \end{bmatrix}, \qquad \hat{\boldsymbol{B}} = \begin{bmatrix} 0 \\ \hat{b}_6 \\ \vdots \\ \hat{b}_0 \end{bmatrix}$$

$$\boldsymbol{C} = [1 \quad 0 \quad \cdots \quad 0] \tag{26}$$

where $\hat{\boldsymbol{e}}$ is the state of the full-order observer, and the control law is given by $u = -\hat{\boldsymbol{K}}_c\hat{\boldsymbol{e}}$, where the feedback gain $\hat{\boldsymbol{K}}_c$ is obtained by solving the ARE

$$\hat{\boldsymbol{A}}^T\boldsymbol{P} + \boldsymbol{P}\hat{\boldsymbol{A}} - \boldsymbol{P}\hat{\boldsymbol{B}}R_c^{-1}\hat{\boldsymbol{B}}^T\boldsymbol{P} + \boldsymbol{C}\boldsymbol{C}^T = \boldsymbol{0} \tag{27}$$

pointwise in time as and when the parameters are estimated. For faster estimation, the eigenvalues of observer dynamics $\hat{\boldsymbol{A}} - \hat{\boldsymbol{K}}_0\boldsymbol{C}^T$ are placed 3 to 5 times farther to the left of those of $\hat{\boldsymbol{A}} - \hat{\boldsymbol{K}}_c\hat{\boldsymbol{B}}$.

In the given adaptive optimal pole-placement feedback law, the stabilizability of the pair $(\hat{\boldsymbol{A}}, \hat{\boldsymbol{B}})$ cannot always be guaranteed at each frozen time t. This problem arises because there is no way to avoid the cancellation of right-half plane poles and zeros without any additional modifications. One of the approaches suggested[27] involves constructing a convex set of all unknown parameters $\in \Re^{2n}$ such that the absolute value of the determinant of the Sylvester matrix of estimated polynomial coefficients is always greater than a certain known a priori lower bound. Knowledge of such a known convex bounded set for higher-order plants is difficult to construct and is rather a strong assumption. In this work, the stabilizability of $(\hat{\boldsymbol{A}}, \hat{\boldsymbol{B}})$ is assumed $\forall t \geq 0$, and the simulation studies presented also validate this assumption.

Simulation Results

The parameters used to approximately represent those of the F-16 aircraft wing/store model with the GBU-8/B weapon system[19] and that are used for the current simulation are $\rho = 0.008256$ slug/ft^3, $m_s = 1027.6$ kg (2265 lb), $x_\alpha b = 0.178$ m (7.04 in.), $m_w = 5.3m_s$, $x_\theta b = 0$, $m_a\ell_a = 13.61$ kg (30 lb), $\ell_1 b = 0.223$ m (8.8 in.), $r_\alpha b = 0.635$ m (25 in.), $\ell_2 b = 0.223$ m (8.8 in.), $r_\theta b = 0.830$ m (32.7 in.), $ab = -0.1702$ m (-6.68 in.), $b = 1.12$ m (44 in.), $\omega_h = 24.5$ rad/s, $\omega_\theta/\omega_h = 0.55$, and $\omega_\alpha/\omega_h = 1.27$. Reference 20 presents some of the open-loop responses illustrating the effectiveness of the decoupler pylon-mounted wing/store flutter suppression system. The open-loop flutter speed with the cited values is found to occur at $U/b = 170$ s^{-1} for the decoupler case, $U/b = 127$ s^{-1} for the rigid case, and $U/b = 148$ s^{-1} for the clean wing (without any store). This represents a 14.86% increase in flutter speed with the decoupler pylon over that of a bare wing and a 33.86% increase over the rigidly attached case.

In the algorithm given in an earlier section, the values assigned to the design variables are the adaptation gain $\boldsymbol{\Gamma} = \boldsymbol{I}_{15}$, the switching parameter $\sigma_0 = 200$, the filter parameter $\lambda_f = 2$, the observer pole factor $\beta = 3$, and the control weighting $R_c = 10$. The simulation consists of the release of a 500-lb-mass bomb from a rack of 2265 lb at the 20th nondimensional time unit.

Figure 5 shows the response of the store pitch angle as a function of time at $U/b = 160$ s^{-1}. It is observed that at the instant

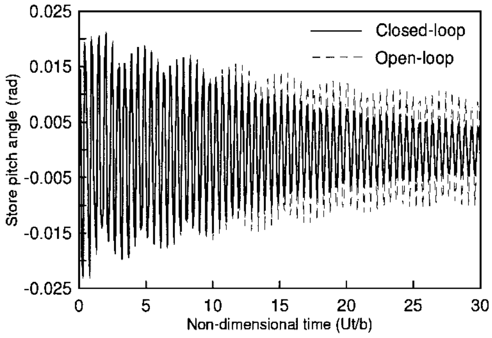

Fig. 5 Open- and closed-loop response of store pitch angle θ at $U/b = 160$ s^{-1}.

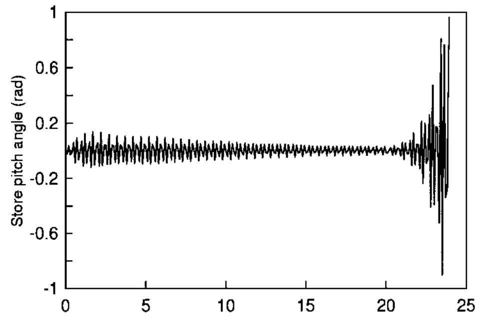

Fig. 6 Unstable open-loop response, θ.

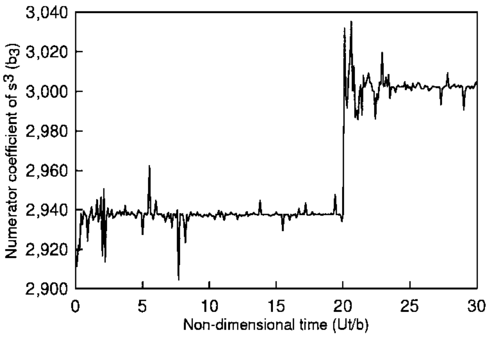

Fig. 7 Estimation of parameter $\psi_4 = b_3$ = coefficient of s^3.

of store release, there is insignificant change in the response. This is because the simulation ensures that the initial conditions of the states at the 20th nondimensional time unit are the values of the states at the 19.9th nondimensional time unit (continuous evolution). When compared to the open-loop response, the closed-loop system demonstrates relatively faster settling time and reduced magnitude of vibration. Note that the closed-loop response plotted in Fig. 5 is with the uncertainty model included, whereas the open-loop response does not include the model. The response of the open-loop with the multiplicative uncertainty model included becomes unstable (Fig. 6) as soon as the system is given a perturbation of the earlier described nature. Also, because only a change in store mass is considered in this analysis during the store release event, there is hardly any observable perturbation in the closed-loop response. In reality, sudden release of store causes simultaneous variations in other parameters, such as center of gravity location of the store, its radius of gyration, etc., in addition to the change in store mass. If the nature of variations of these parameters with the change in store mass is known, then a comprehensive analysis could perhaps be performed to further investigate a more realistic situation.

A very obvious change is seen in the parameter estimation response, where the estimated parameters are the coefficients of the numerator and denominator polynomials, totaling 15. A representative plot of a parameter from numerator (coefficient of s^3) is shown in Fig. 7. With the initial values for these coefficients being different, the search for the true parameters takes place, with the true parameters being the coefficients corresponding to 2265-lb mass. At the

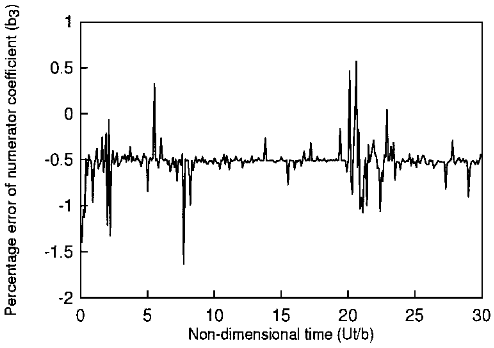

Fig. 8 Percentage estimation error of $\psi_4 = b_3$ = coefficient of s^3.

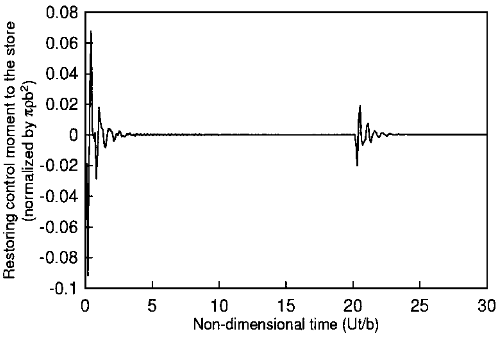

Fig. 9 Control authority.

instant of store release, the true and unknown mass suddenly jumps to 1765 lb. This is clear from the step change in the estimated parameter response at the 20th nondimensional time unit. Again the search process continues as before, as governed by the adaptation law.

Figure 8 shows the percentage error between the true unknown parameter and the estimated parameter values corresponding to the coefficient shown in Fig. 7. It is observed that the percentage errors are negligible, which leads to the conclusion the adaptation is effective in estimating the unknown parameters.

The corresponding control history ($u = -\hat{\boldsymbol{K}}_c\hat{\boldsymbol{e}}$) is shown in Fig. 9, where the peak value of the control effort is around 0.06 units. At the instant when the store is released, the actuator response shows signs of perturbation in its simulation. This is because the control effort is being put in to the system to estimate and control the unknown parameters back. It remains to be seen (work in progress) whether the peak value is within the limits of actuator saturation value. If it is not, then the control weighting λ_f can appropriately be modified to accommodate for the limitations.

Conclusions

An indirect adaptive robust control algorithm-based controller is designed for a single-input/single-output wing/store model. The algorithm consists of an adaptive law that is based on gradient method modified (with leakage and switching-σ algorithms) to make the closed-loop system robust to modeling uncertainties and parameter variations. The feedback control loop consists of a linear quadratic adaptive controller that uses the estimated plant parameters to construct a state observer gain matrix. LQR law is then used to construct the state feedback gain matrix adaptively.

The effectiveness of the designed adaptive controller is verified by simulating a sudden change in store mass parameter (at subcritical flutter speed) representing the real-life situation of an ejection of a bomb out of an underwing external rack. The online estimator performed very well in tracking the uncertain plant parameter coefficients to a small percentage error of their true value. The controller also demonstrated an improvement in performance over the open-loop response in terms of faster settling time and smaller steady-state amplitude. Moreover, the presence of an input multiplicative uncertainty model had no effect on the stability of the closed-loop system whereas it caused the open-loop system response to diverge. This type of robustness is especially critical during combat maneuvers.

Acknowledgment

The authors are grateful for the generous support of the U.S. Air Force Office of Scientific Research Grant AFOSR-F49620-95-1-0362 under the direction of Brian Sanders.

References

[1]Mykytow, W. J., "Recent Analysis Methods for Wing/Store Flutter," *Specialist Meeting on Wing-with-Stores Flutter*, AGARD-CP-162, April 1962.

[2]Katz, H., "Flutter of Aircraft with External Stores," *Proceedings of Aircraft Stores Symposium*, Vol. 2, Armament Development and Test Center, Eglin AFB, FL, Nov. 1969.

[3]Foughner, J. T., Jr., and Besinger, C. T., "F-16 Flutter Model Studies of External Wing Stores," NASA-TM-74078, Oct. 1977.

[4]Triplett, W. E., "A Feasibility Study of Active Wing/Store Flutter Control," *Journal of Aircraft*, Vol. 9, No. 6, 1972, pp. 438–444.

[5]Noll, T. E., Felt, L. R., Mykytow, W. J., Russell, H. L., and Major, H. L., "Potential Application of Active Flutter Suppression to Future Fighter Attack Aircraft," Aircraft/Stores Compatibility Symposium, U.S. Air Force Flight Dynamics Lab., Sept. 1973.

[6]Sandford, M. C., Abel, I., and Gray, D. L., "Development and Demonstration of a Flutter Suppression System Using Active Controls," NASA-TR-R-450, Dec. 1975.

[7]Harvey, C. T., Johnson, T. L., and Stein, G., "Adaptive Control of Wing/Store Flutter," AFFDL-TR-79-3081, U.S. Air Force Flight Dynamics Lab., Wright–Patterson, OH, April 1979.

[8]Haidl, G., Lotze, A., and Sensburg, O., "Active Flutter Suppression on Wings with External Stores," AGARD-AG-175, 1974.

[9]Hönlinger, H., "Active Flutter Suppression on an Airplane with Wing Mounted External Stores," AGARD-CP-228, 1978.

[10]Hönlinger, H., and Destuynder, R., "External Store Flutter Suppression with Active Controls," *Lecture Series, von Kármán Institute for Fluid Dynamics*, Vol. 2, Dec. 1978, pp. 1–85.

[11]Reed, W. H., III, Foughner, J. T., Jr., and Runyan, H. L., "Decoupler Pylon: A Simple Effective Wing/Store Flutter Suppressor," *Journal of Aircraft*, Vol. 17, No. 3, 1980, pp. 206–211.

[12]Triplett, W. E., Kappus, H. P. F., and Landy, R. J., "Active Flutter Suppression Systems for Military Aircraft—A Feasibility Study," AFFDL-TR-72-116, U.S. Air Force Flight Dynamics Lab., Wright–Patterson, OH, Feb. 1973.

[13]Runyan, H. L., "Effect of a Flexibly Mounted Store on the Flutter Speed of a Wing," NASA-CR-159245, April 1980.

[14]Desmarais, R. N., and Reed, W. H., III, "Wing/Store Flutter with Nonlinear Pylon Stiffness," *Journal of Aircraft*, Vol. 18, No. 11, 1981, pp. 984–987.

[15]Lottati, I., "Aeroelastic Tailoring of a Composite Wing with a Decoupler Pylon as a Wing/Store Flutter Suppressor," *Journal of Aircraft*, Vol. 25, No. 3, 1988, pp. 271–280.

[16]Yang, Z.-C., and Zhao, L.-C., "Wing-Store Flutter Analysis of an Airfoil in Incompressible Flow," *Journal of Aircraft*, Vol. 26, No. 6, 1989, pp. 583–587.

[17]Yang, Y.-R., "KBM Method of Analyzing Limit Cycle Flutter of a Wing with an External Store and Comparison with a Wind-Tunnel Test," *Journal of Sound and Vibration*, Vol. 187, No. 2, 1995, pp. 271–280.

[18]Peloubet, R. P., Jr., Haller, R. L., and McQuien, L. J., "Feasibility Study and Conceptual Design for Application of NASA Decoupler Pylon to the F-16," NASA CR-165834, May 1982.

[19]Clayton, J. D., Haller, R. L., and Hassler, J. M., Jr., "Design and Fabrication of the NASA Decoupler Pylon for the F-16 Aircraft," NASA CR-172354, Jan. 1985.

[20]Gade, P. V. N., and Inman, D. J., "Two-Dimensional Active Wing/Store Flutter Suppression Using $\mathcal{H}_\infty$ Theory," *Journal of Guidance, Control, and Dynamics*, Vol. 20, No. 5, 1997, pp. 949–955.

[21]Gade, P. V. N., and Flowers, G. T., "Flutter Suppression of an Airfoil with Unsteady Forces Using a Piezoelectric Active Strut," AIAA Paper 94-1746, April 1994.

[22]Pokines, B., Belvin, W. K., and Inman, D. J., "Static and Dynamic Characteristics of a Piezoceramic Strut," 5th AIAA/DOD Control–Structures Interaction Technology Conf., Lake Tahoe, NV, 1992, pp. 133–140.

[23]Theodorsen, T., "General Theory of Aerodynamic Instability and the Mechanism of Flutter," NACA Rept. 496, 1935.

[24]Edwards, J. W., "Unsteady Aerodynamic Modeling and Active Aeroelastic Control," Stanford Univ., SUDAAR 504, Stanford, CA, Feb. 1977.

[25]Jones, R. T., "Operational Treatment of the Nonuniform Lift Theory to Airplane Dynamics," NACA TN 667, 1938.

[26]Zhou, K., Doyle, J. C., and Glover, K., *Robust and Optimal Control*, Prentice–Hall, Upper Saddle River, NJ, 1996.

[27]Ioannou, P. A., and Sun, J., *Robust Adaptive Control*, Prentice–Hall, Upper Saddle River, NJ, 1996.

[28]Slotine, J.-J. E., and Li, W., *Nonlinear Control Theory*, Prentice–Hall, Englewood Cliffs, NJ, 1991.